

Characterization of fossil remains using XRF, XPS and XAFS spectroscopies

This content has been downloaded from IOPscience. Please scroll down to see the full text.

2016 J. Phys.: Conf. Ser. 712 012090

(<http://iopscience.iop.org/1742-6596/712/1/012090>)

View [the table of contents for this issue](#), or go to the [journal homepage](#) for more

Download details:

IP Address: 155.207.11.190

This content was downloaded on 02/06/2016 at 09:20

Please note that [terms and conditions apply](#).

Characterization of fossil remains using XRF, XPS and XAFS spectroscopies

I M Zougrou¹, M Katsikini^{1*}, F Pinakidou¹, M Brzhezinskaya², L Papadopoulou³,
E Vlachos³, E Tsoukala³ and E C Paloura¹

¹ School of Physics, Aristotle University of Thessaloniki, 54124 Thessaloniki, Greece.

² Main Department Scientific-Technical Infrastructure II, Helmholtz Zentrum Berlin, 12489 Berlin, Germany.

³ School of Geology, Aristotle University of Thessaloniki, 54124 Thessaloniki, Greece.

*E-mail: katsiki@auth.gr

Abstract. Synchrotron radiation micro-X-Ray Fluorescence (μ -XRF), X-ray photoelectron (XPS) and X-ray Absorption Fine Structure (XAFS) spectroscopies are applied for the study of paleontological findings. More specifically the costal plate of a gigantic terrestrial turtle *Titanochelon bacharidisi* and a fossilized coprolite of the cave spotted hyena *Crocota crocota spelaea* are studied. Ca $L_{2,3}$ -edge NEXAFS and Ca 2p XPS are applied for the identification and quantification of apatite and Ca containing minerals. XRF mapping and XAFS are employed for the study of the spatial distribution and speciation of the minerals related to the deposition environment.

1. Introduction

The investigation of fossil remains provides valuable information on the evolution of living species, the fossilization conditions and the palaeoenvironment. The aim of this work is to demonstrate the potential of X-ray spectroscopies for the investigation of specimens of paleontological interest. More specifically, Ca $L_{2,3}$ -edge near edge X-ray absorption fine structure (NEXAFS) and X-ray photoelectron (XPS) spectroscopies are applied in combination with extended X-ray absorption fine structure (EXAFS) spectroscopy, X-ray fluorescence (XRF) mapping and more commonly used techniques such as optical microscopy (OM) and scanning electron microscopy (SEM) for the assessment of diagenesis of two different types of paleontological remains: a hyena coprolite and a giant tortoise costal plate. The Ca $L_{2,3}$ -edge NEXAFS and Ca 2p photoelectron spectra provide quantitative information concerning the bone apatite and Ca-rich secondary phases [1-2]. OM and SEM are used to assess the morphology and chemical composition of the coprolite matrix and inclusions, whereas XRF maps were recorded to acquire complementary information on the distribution of P, Ca, Mn and Fe in the specimens [3-4]. Finally, Fe K -edge EXAFS was used to investigate metal-rich inclusions in the coprolite matrix.

2. Materials and methods

The studied fossils are a costal plate of the gigantic Pliocene tortoise *Titanochelon bacharidisi* from the New Michaniona, Thessaloniki, Greece, [5] excavation site found in open air as a result of sea erosion and a fossilized coprolite (SKG914) of the Late Pleistocene cave spotted hyena *Crocota*



crocuta spelaea from the Agios Georgios cave in Kilkis, Greece [6]. The XRF, XPS and XAFS measurements were conducted at the BESSY-II Synchrotron Radiation Storage Ring of the Helmholtz Zentrum Berlin. The XRF maps and the Fe *K*-edge XAFS spectra were recorded on the samples' cross sections at the KMC-II beamline using an energy dispersive silicon detector positioned on the horizontal plane at right angle to the incident beam that was impinging at 45° to the sample surface. For the acquisition of the XRF maps, the beam diameter was reduced to 4.8 μm using an elliptical capillary and the energy of the excitation beam was set equal to 7.2 keV. The maps were corrected for the escape peak contributions. The X-ray photoelectron and Ca *L*_{2,3}-edge NEXAFS spectra were recorded at the Optics beamline (PM-4) using the SURICAT end-station and at the Russian German beamline (RGLB) under ultrahigh vacuum conditions. The fossil remains were powdered and then rubbed onto a scratched pure In foil to minimize charging effects. The beam with spot size of 0.1×0.5 mm was impinging at 45° to the sample. The X-ray photoelectron spectra were recorded with excitation photon energy of 1030 eV using a hemispherical capacitor electron energy analyzer (Scienta SES 100) with energy resolution of 160 meV. Energy shifts due to charging effects were corrected by setting the C 1s peak at 284.6 eV. The Ca *L*_{2,3}-edge NEXAFS spectra were recorded in the total electron yield mode measuring the drain current from the sample.

3. Results and discussion

Representative OM, SEM-back-scattering electron (BSE) images, and XRF maps of the coprolite specimen are shown in figure 1. SEM- energy dispersive X-ray spectra (EDS) were used for the determination of the chemical composition. The dominant phase was identified as a non-apatitic calcium phosphate matrix with average Ca/P atomic ratio of 1.55±0.11. Furthermore, bone inclusions with well-preserved Haversian bone histology with visible osteocyte lacunae as well as grains of quartz, green hornblende [(K,Na)₀₋₁Ca₂(Mg,Fe,Al)₅(Si,Al)₈O₂₂(OH)₂], biotite [K₂(Mg,Fe)₃AlSi₃O₁₀(OH)₂], almadine/glossular garnet [(Ca,Fe)₃Al₂Si₃O₁₂] and microcline (KAlSi₃O₈) were also identified throughout the specimen. The latter inclusions are related to minerals introduced from the deposition environment. The primary carbonated hydroxylapatite (HA) of the bone is found enriched in K, Na, Rb, Sr and partially transformed to chlorapatite. The average Ca/P atomic ratio of bone inclusions is similar to HA and equal to 1.65±0.11. In the Ca and P XRF maps, local maxima related to the bone inclusions are observed. However, in areas of low Ca and P intensity, metal-rich (Fe, Mn) inclusions originating from the deposition environment are also present.

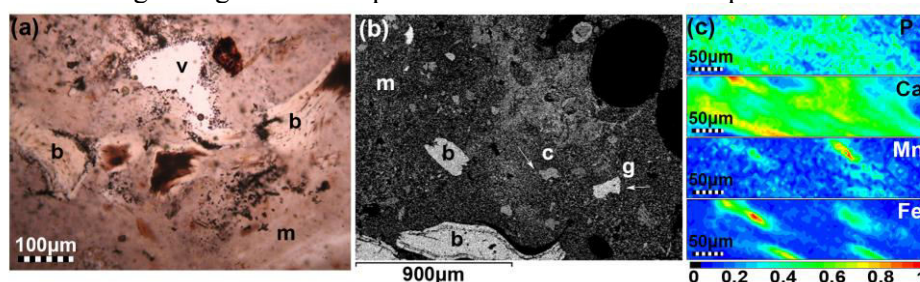


Figure 1. Coprolite specimen: a) OM image recorded using plane polarized light that shows digested bone with visible osteocyte lacunae, b) SEM-BSE image revealing grain and bone inclusions in the spotted cave hyena coprolite matrix (SGK 914), c) P, Ca, Mn and Fe XRF maps identify elongated metal-rich inclusions in areas of low Ca and P concentration. *Notation:* b: bone, m: matrix, v: vesicle, c: microcline, g: glossular garnet.

The Fe *K*-edge XANES spectrum recorded in the cross section of the coprolite, reveals that Fe is in the trivalent state, as it is deduced from the position of the absorption edge. The amplitude of the Fourier transform of the *k*³-weighted $\chi(k)$ Fe *K*-edge EXAFS spectrum is shown in figure 2 along with the $\chi(k)$ spectrum shown in the inset. Fitting of the spectrum using the FEFF8 package [7] reveals that

Fe participates in the formation of the akaganeite mineral. More specifically, 6 O atoms comprise the first nearest neighbouring shell at 1.99 Å, 4 and 4 Fe atoms, at distances 3.09 (edge-sharing) and 3.42 (corner-sharing) Å, respectively, constitute the second shell while the 4th nearest neighbouring shell consists of 6 O atoms located at 3.70 Å.

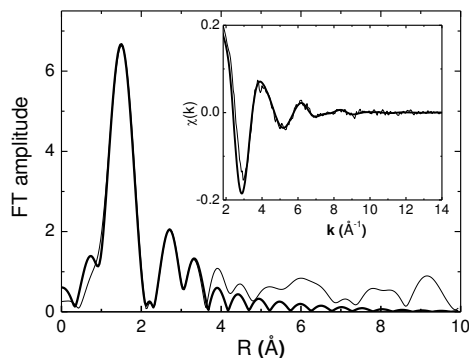


Figure 2. Fe *K*-edge $\chi(k)$ (inset) and corresponding amplitude of the Fourier Transform of the k^3 -weighted $\chi(k)$ spectra of the hyena coprolite. The experimental spectra and the fitting curves are shown in thin and thick lines, respectively.

Ca $L_{2,3}$ -edge NEXAFS and Ca 2p X-ray photoelectron spectra were used to investigate the chemical composition of the gigantic tortoise external cortex and cancellous bone as well as the hyena coprolite. To obtain quantitative information, the Ca $L_{2,3}$ -edge NEXAFS spectra were fitted using Sigmoidal and Voigt functions as shown in figure 3. A photograph of the gigantic tortoise sample cross section is shown in the inset. The corresponding spectra of reference HA, chlorapatite (ChAp) and calcite samples are also included in figure 3. The fitting results are listed in table 1 along with HA and calcite results from Benzerara *et al.* (2004) [8]. The energy splitting of the (a_2 - a_1) and (b_2 - b_1) peaks is used for the identification of the Ca-containing minerals. The giant tortoise external cortex consists of HA whereas the cancellous bone is comprised of 65% HA and 35% calcite. The coprolite spectrum shows the presence of chlorapatite.

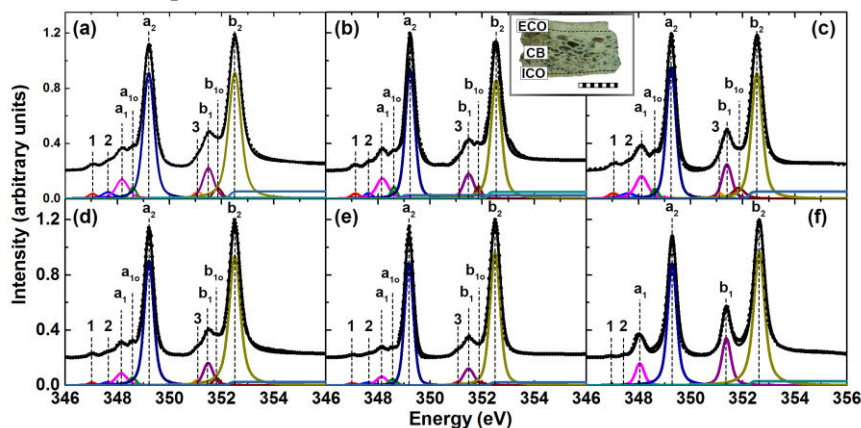


Figure 3. Ca $L_{2,3}$ -edge NEXAFS spectra (dotted lines) and fitting curves (solid lines) using sigmoidal steps and Voigt peaks of the: (a) hyena coprolite, (b) giant tortoise external cortex, (c) giant tortoise cancellous bone and reference (d) hydroxylapatite, (e) Norway chlorapatite and (f) calcite samples. The experimental and fitting lines are shifted along the y-axis for clarity. A photograph of the giant tortoise costal plate cross section is shown in the inset. The external cortex (ECO), cancellous bone (CB) and internal cortex (ICO) are indicated. *Scale bar:* 1 cm.

Similar to the case of the Ca $L_{2,3}$ -edge NEXAFS spectra, Ca 2p XPS spectra are also sensitive to the chemical state of Ca. The spectrum of the giant tortoise cancellous bone is shown in figure 4. It is fitted using two doublets, each one for HA and calcite contributions, with full width at half maximum of 2.20 and 3.27 eV, respectively. The relative contributions of the HA and calcite phases is found equal to 64% and 36%, respectively, in accordance with the NEXAFS results.

Table 1. Fitting results of the Ca $L_{2,3}$ -edge NEXAFS spectra of the giant tortoise compact and cancellous bone and the hyena coprolite. Fitting results of the reference spectra of HA, geologic Norway chlorapatite (ChAp) and calcite as well as the peak positions of a mixed 65% HA and 35% calcite model are also included. The error in the determination of the peak positions is ± 0.03 eV.

Peak	Tortoise compact	Tortoise cancellous	Hyena Coprolite	HA	HA ^[8]	Norway ChAp	Calcite	Calcite ^[8]	mixed model
1	347.13	347.03	347.05	347.02	347.1	347.02	346.92	346.9	346.99
2	347.63	347.60	347.64	347.62	347.7	347.63	347.45	347.4	347.56
a₁	348.16	348.11	348.18	348.15	348.2	348.14	348.05	348.0	348.12
a₁₀	348.61	348.63	348.59	348.58	348.6	348.57			348.58
a₂	349.23	349.25	349.21	349.21	349.3	349.19	349.29	349.3	349.24
3	351.10	351.08	351.08	351.07		351.07			351.07
b₁	351.48	351.39	351.50	351.48	351.6	351.48	351.37	351.4	351.44
b₁₀	351.85	351.84	351.85	351.81	351.8	351.86			351.81
b₂	352.53	352.54	352.51	352.50	352.5	352.49	352.63	352.6	352.55
a₂-a₁	1.07	1.13	1.03	1.06	1.1	1.05	1.24	1.3	1.12
b₂-b₁	1.05	1.15	1.01	1.02	0.9	1.01	1.26	1.2	1.10
b₂-a₂	3.30	3.29	3.30	3.29	3.2	3.30	3.34	3.3	3.31

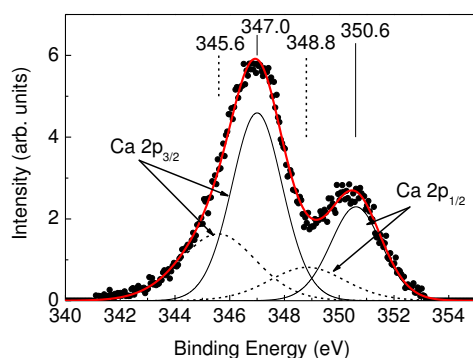


Figure 4. High resolution Ca 2p X-ray photoelectron spectrum of cancellous bone from the gigantic tortoise sample. Fitting using peaks that correspond to HA and calcite contributions are plotted in solid and dashed lines, respectively. The experimental and fitting curves are plotted with solid circles and thick solid (red) line, respectively.

4. Conclusions

Ca $L_{2,3}$ -edge NEXAFS and XPS spectroscopies can provide quantitative information on the Ca chemical state and thus are useful tools for addressing questions of taphonomic interest on bone alterations. OM, SEM, XRF and EXAFS can provide complementary information on the morphology and chemical composition of fossil remains that is strongly affected by the deposition environment.

Acknowledgements

The measurements at the electron storage ring BESSY II (HZB) were financially supported from the European Community's Seventh Framework Program (FP7/2007-2013) under grant agreement n.°312284. Dr. R. Ovsyannikov is also greatly acknowledged for his support at the Optics beamline.

References

- [1] Cosmidis *et al.* 2015 *Acta Biomater.* **12** 260-269.
- [2] Nakada *et al.* 2012 *International Journal of Biomaterials* **2012** ID 615018
- [3] Zougrou I M *et al.* 2014 *J. Synchr. Rad.* **21** 149–160.
- [4] Zougrou I M *et al.* 2014 *J. Phys. Conf. Ser.* **499** 012015.
- [5] Vlachos E *et al.* 2014 *J. Vertebrate Paleontology* **34** 560.
- [6] Tsoukala E S 1992 *Geobios*, **25** 415.
- [7] Ankudinov A L *et al.* 1998 *Phys. Rev. B* **58** 7565–7576
- [8] Benzerara K *et al.*, 2004, *Geobiology* **2** 249-259.